

Resonant slot optical guiding in metallic nanoparticle chains

K. J. Webb* and J. Li

School of Electrical and Computer Engineering, Purdue University, West Lafayette, Indiana 47907, USA

(Received 12 July 2005; published 18 November 2005)

The process by which a closely spaced array of metallic nanoparticles can effectively guide light by means of an interparticle slot which is resonant in the dimension transverse to the chain direction is described. Specific geometries related to the material parameters produce a resonance in a waveguide mode existing between rectangular particles, and this has a dramatic impact on the guiding properties. Use of a model for this resonant transfer permits the design of waveguides which can operate with relatively low loss using this new guiding mechanism.

DOI: [10.1103/PhysRevB.72.201402](https://doi.org/10.1103/PhysRevB.72.201402)

PACS number(s): 73.20.Mf, 78.67.Bf, 42.79.Gn, 42.82.Et

After the guiding of light by a linear chain of silver nanoparticles was proposed and simulated,¹ a number of ensuing experimental studies confirmed the concept.²⁻⁵ This type of waveguide has enhanced the prospects for small-scale optical integrated circuits because the light is confined near the nanoparticles, which have dimensions of tens of nanometers. There are also many interesting spectroscopy applications, as molecules can be attached to the nanoparticles and the interaction length and geometry provided by the waveguide could enhance sensitivity to, for example, Raman scattered light. More generally, light in nanoscale structures offers opportunities in near-field optics.⁶

The nanoparticle chain has been understood to operate as a concatenation of elements, each of which is under a Mie-type small particle resonance, and hence the metal parameters dictate the best operating wavelength.¹ In the small particle Mie resonance limit, where the resonant frequency depends on the material properties only, absorption dominates scatter and field penetration into the particle is significant. Furthermore, closely spaced particles will interact strongly. It has been suggested that an analog exists in the microwave frequency range, where coupling of wires that is well understood from antenna arrays could be relevant.⁷ However, the material properties of metals differ significantly between the microwave and visible/infrared portions of the spectrum. The distances between particles in the waveguide chains is typically small relative to the free space and plasmon-polariton surface wave wavelengths, placing them far from a photonic crystal band gap.^{1,3} The interaction between nanoparticles has been ascribed to a change in the particle polarization associated with an ensemble surface plasmon.⁵ Also, measurements of the scattering cross sections for individual particles and collections of particles have shown a red shift in, for example, the scattering resonance from dimers. However, none of these physical descriptions explain why the field has been observed to be primarily located between the nanoparticles in a chain² or how the field is modulated along the chain,⁸ nor how particle geometry relates to desirable waveguide characteristics. We provide a description of the nanoparticle waveguide that allows us to explain the fundamental guiding principle in terms of a resonant gap field. This view provides a new form of guiding, and our analytic description allows structures to be designed for low loss operation.

In the visible and infrared portions of the spectrum, noble metals such as silver (Ag) and gold (Au) are good reflectors, having plasma resonances in the ultraviolet. For particles sufficiently large, bulk dielectric constants (ϵ) apply,⁹ and we assume this regime. The negative real part of the dielectric constant in metals over much of the visible and infrared spectrum allows a surface or a strip to guide a wave.¹⁰ As the plasma frequency is approached, intrinsic material losses become significant.

We consider the rectangular two-dimensional (2D) nanoparticle chain shown in Fig. 1, where the gap between the metal particles (slot width d) is considered small relative to the particle length (p). Figure 2 shows a finite element simulation for $|H_y(x, z)|$ for a Ag nanoparticle chain that is acting as a waveguide. Remarkable is the field confinement afforded by the slots between the particles. The wavelength used is 381.49 nm in the background, which is assumed to be free space ($\epsilon_d=1$), and the Ag nanoparticle has $\epsilon_m=-3.47+i0.19$. The chain has 20 particles, each with $p=30$ nm and $w=33.1$ nm, and the separation (slot width) is $d=15$ nm. The excitation is at the first particle on the left, and $\hat{n} \times \mathbf{H}=1$ is enforced on the boundary with $\mathbf{H}=0$ inside, i.e., the electric current density in the constant- y plane is $J_s=1$ A/m.

A strip waveguide result is shown in Fig. 3 for comparison with the chain waveguide. The same excitation was used as for the chain, i.e., there is a separate nanoparticle at the left which is excited, and the strip length is equal to that for the remaining 19 nanoparticles with gaps. While the effective excitation in the two cases is not identical, because the strip and particles present slightly different source loads, we do

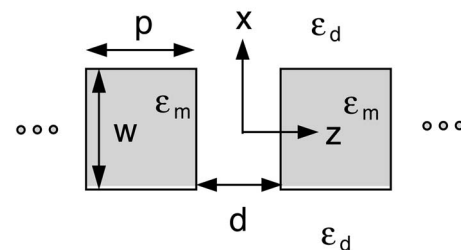


FIG. 1. A metal nanoparticle chain waveguide geometry, where ϵ_m is the dielectric constant of the metal and ϵ_d is the dielectric constant of the background.

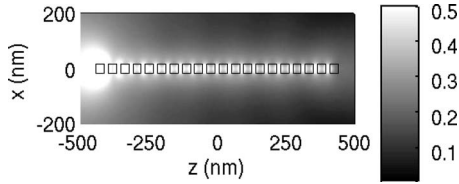


FIG. 2. $|H_y|$ for a 20 element Ag nanoparticle chain waveguide. Parameters: $\lambda_d=381.49$ nm, $\epsilon_d=1$, $\epsilon_m=-3.47+i0.19$, $p=30$ nm, $w=33.1$ nm, and $d=15$ nm. Excitation is at the particle on the left.

not expect that this difference is significant. The standing wave pattern in Fig. 3 indicates a single propagating mode and results from the reflection at the strip termination (right-hand end). Notice that at some distance from the chain waveguide in Fig. 2, there also appears to be a similar standing wave pattern. Note also that the nanoparticle waveguide has a much larger and more confined field than the strip waveguide.

The regions between the slots in Fig. 1 are uniform strip waveguides, and the guided fields can be represented as a set of uniform waveguide solutions. We show that for small d , the dominant nanoparticle waveguide mode phase constant is approximately that for the lowest order uniform strip mode. With sufficiently small field penetration (skin depth) relative to the particle dimension (p), the regions between the particles can be treated as slot waveguides in an infinite metal film. This allows an approximate calculation of the slot fields, which for small d are dominated by a single propagating mode that does not cut off with reducing d . It is resonance in this gap mode which we have found provides significant guiding features. Others have thought of the nanoparticle chain in terms of the single particle, with coupling. We provide a totally different view and regime, where transverse resonance in the gap mode is critical.

In studying the nanoparticle chain, it is therefore instructive to consider waveguide modes for the metal strip or slot (with the approximation that $p \rightarrow \infty$) geometry of Fig. 4. These problems have an analytic set of eigenmodes¹⁰ and can be treated using the same formalism. For wavelengths sufficiently far from the plasma resonance, the eigenvalues are approximately those for lossless material with either electric wall ($\hat{\mathbf{x}} \times \mathbf{E} = 0$ at $x=0$) or magnetic wall ($\hat{\mathbf{x}} \times \mathbf{H} = 0$ at $x=0$) symmetry. For the metal, $\epsilon_m < 0$, and for the dielectric, $\epsilon_d > 0$. The transverse resonant field solution gives the same eigenvalue equation for the strip and slot. Using the coordinate system for the strip from Figs. 1 and 4 (where x is the transverse variable and z the direction of propagation), the eigenvalues can be found from

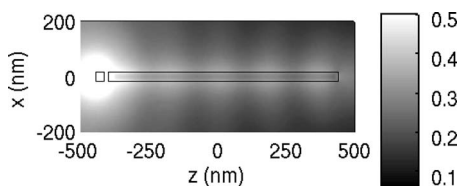


FIG. 3. $|H_y|$ for a Ag strip waveguide. The excitation and relevant parameters are as in Fig. 2.

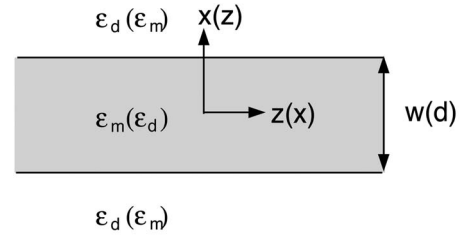


FIG. 4. Metal strip (of width w) or slot (of width d) waveguide geometry, where the dimensional and material parameters are as in Fig. 1.

$$Z_{xm} \frac{Z_{xd} + Z_{xm} \tanh(-ik_{xm}w/2)}{Z_{xm} + Z_{xd} \tanh(-ik_{xm}w/2)} \rightarrow \begin{cases} 0 \\ \infty \end{cases}, \quad (1)$$

where $k_{xm} = \sqrt{k_m^2 - k_z^2}$, with $k_m = \omega \sqrt{\epsilon_m}/c$, and Z_x is the x -directed wave impedance. For the TM case, $Z_{xi} = k_{xi}/(\omega \epsilon_i \epsilon_0)$, where $i=m$ or d , and ϵ_0 is the permittivity of free space. Figure 5 gives the normalized dispersion curves for propagating strip modes, k_z/k_d , where $k_d(\omega) = \omega \sqrt{\epsilon_d}/c$ is the wave number for the dielectric region, as a function of normalized strip width, w/λ_d , where λ_d is the wavelength in the dielectric. Figure 5 also gives k_x/k_d for the slot as a function of normalized slot width, d/λ_d , referring to the geometry of Figs. 1 and 4. With $\epsilon_d=1$, the $\epsilon_m/\epsilon_d=-3.47$ curves corresponds to Ag without loss at a wavelength of 381.49 nm, and $\epsilon_m/\epsilon_d=-14.88$ to 582.08 nm. The important feature to note regarding the slot (and strip) dispersion curves is that there is a TM (H_y, E_x, E_z) propagating mode for arbitrarily small width.

The large fields in the slot region between each particle occur with resonance (in the x -direction, referring to Fig. 1) of the dominant propagating mode. Given the particle separation d , resonance occurs with $w = l_f + n\lambda_x/2$, where l_f is the cavity length for the fundamental mode resonance, $n=0, 1, 2, \dots$, and $\lambda_x = 2\pi/k_x$ is the dominant slot mode wavelength. Assuming the field penetration into the particle is small relative to the dimension p , the slot mode eigenvalue can be found from Fig. 5.

For the case shown in Fig. 2, the value for w has been adjusted for the first resonance of the slot mode, and beyond the excitation region energy does not flow perpendicular to the chain direction. The propagating slot mode for the lossless case, from Fig. 5, has $k_x/k_d=3.15$ (referring to the ge-

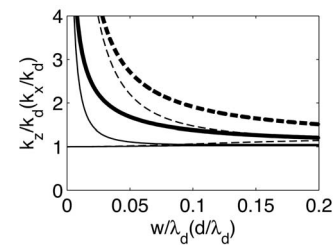


FIG. 5. Eigenvalue solutions for strip (k_z/k_d) and slot (k_x/k_d) waveguides, referring to Fig. 4. The thin lines are for the metal strip case and the thick lines the slot case. Parameters: $\epsilon_m/\epsilon_d=-3.47$ (dashed); $\epsilon_m/\epsilon_d=-14.88$ (solid).

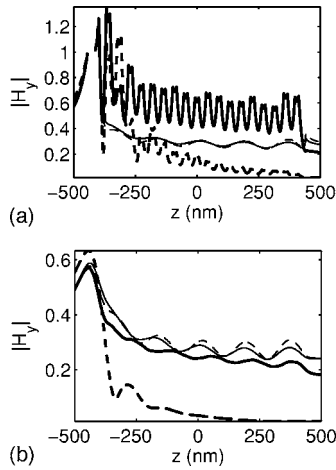


FIG. 6. $H_y(z)$ (a) in the center ($x=0$) and (b) at 40 nm above the top surface of the waveguides. Parameters: as in Fig. 2; thick (nanoparticle chain); thin (strip); $w=33.1$ nm (solid); $w=40.0$ nm (dashed).

ometry of Fig. 1) and hence $\lambda_x/2=60.58$ nm. The value of w in Fig. 2 (33.1 nm) is less than $\lambda_x/2$ because of the near-field or reactance at the slot termination planes ($x=\pm w/2$) and the impact of field penetration into the particle on k_x (the skin depth in this case is 30 nm). With significant field penetration, a better estimate for the dominant mode k_x in the slot comes from a periodic field solution in z .

Figure 6 gives $|H_y(z)|$ from Fig. 2 along the centerline of the chain and strip waveguides ($x=0$) and 40 nm above the top surface of the waveguides. In Fig. 6(a), note the dramatic difference in amplitude and confinement between the resonant nanoparticle case ($w=33.1$ nm) and the off-resonant example ($w=40$ nm). In both cases, but more evident on resonance, the field is larger between the particles ($z=0$ corresponds to a gap center, where an electric wall occurs, and the transverse constant- z plane through the particle center is a magnetic wall). While there is some decay away from the source, this is most significant when the slot fields are not resonant. Figure 6(b) shows that both the chain and the strip have the same single mode standing wave period when measured sufficiently far from the surface. The shift in this pattern for the chain relative to the strip is due to the differing effective reflection coefficient (phase) for the field at the termination of the waveguide.

The fields in the slot between the 10th and 11th particles, at $z=0$, and along the centerline of the 11th particle, are given in Figs. 7(a) and 7(b), respectively. In the slot, E_z is a maximum at the top and bottom, and H_y is maximum in the center ($x=0$), indicating an approximate magnetic wall at the top and bottom and an electric wall at the center. The mode that is excited by the source has odd $E_z(x)$ and even $H_y(x)$. Moving the slot length (particle width w) just slightly off resonance significantly reduces the field. Wide slots (larger d) will have lower quality factor, less field enhancement, and less sensitivity to geometry variations. Figure 8 gives $|H_y(x)|$ averaged from the 4th to the 18th particle, to remove local standing wave effects and allow a comparison of the effective field confinement in the chain and strip waveguides. In-

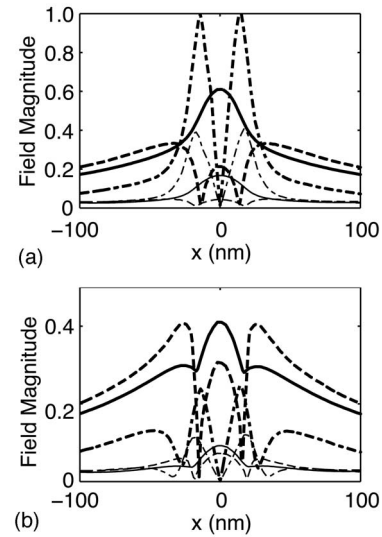


FIG. 7. The magnitude of $H_y(x)$, $E_x(x)$, and $E_z(x)$ for (a) $z=0$, the centerline between the 10th and 11th particles, and (b) $z=22.5$ nm, the centerline of the 11th particle: $|H_y(x)|$ (solid); $|E_z(x)|$ (dashed-dotted); $|E_x(x)|$ (dashed). Parameters: as in Figs. 2 and 6; $w=33.1$ nm (thick); $w=40.0$ nm (thin).

deed, as we can judge from Fig. 2, the chain waveguide has significantly better field confinement than the strip.

Considering the chain waveguide as a series of nanoparticles interacting through their polarization dipole moment does not capture the resonant slot character we have presented, a feature that makes these waveguides uniquely different from the strip and weakly interacting particle cases. As the slot width (d) becomes small, the chain waveguide dominant mode approaches that for the strip waveguide. Physically, the chain has a series of slots that are excited by the intervening strip and which contribute to the collective waveguide action positively when resonant and detrimentally when not resonant.

Assuming a periodic lossless 2D nanoparticle waveguide, a plane wave field expansion valid for $|x|>w/2$ is

$$H_y(x,z) = \sum_{n=-\infty}^{\infty} \int_{k_x} \tilde{H}_y(k_x, k_z) \times \exp[i(k_{z0} + 2n\pi/\Lambda)z] \exp(ik_x x) dk_x, \quad (2)$$

where $\Lambda(=p+d)$ is the period, k_{z0} is the first Brillouin zone

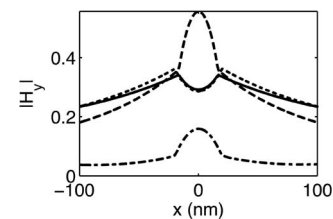


FIG. 8. $|H_y(x)|$ averaged from the 4th to the 18th particle. Parameters: as in Figs. 2 and 6; $w=33.1$ nm chain (dashed); $w=40.0$ nm chain (dashed-dotted); $w=33.1$ nm strip (solid); $w=40.0$ nm (dotted).

eigenvalue, which for a small slot width is given approximately by the strip eigenvalues of Fig. 5, and from the dispersion relation, $k_x = \sqrt{k_d^2 - k_z^2}$. For wave guiding in the z -direction, $k_x = i\alpha_x$. Terms with $|n| > 0$ in (2) result in large α_x and hence rapidly decaying evanescent fields. As a consequence of this, and the relatively small d , the single mode phase constant for the chain some distance above the particles [see Fig. 6(b)] is consistent with that for the strip waveguide. Note that the chain waveguide is far from a band gap, where $k_z \Lambda \sim \pi$.

The dominant wave in the chain waveguide has a wavelength $\lambda_z \gg \Lambda$. This places the structure in the same regime as that which has been assumed for corrugated waveguides.¹¹ In a similar fashion, the field at the top surface of the particles can be represented using a periodic boundary condition comprised of impedances resulting from an electric wall at $x=0$ and transformations through the slot and the particles, creating in the lossless case a reactive boundary condition at the top of the slots and particles that, under conditions of resonance, more effectively confines the field to this boundary than in the strip case.

We have described a new guiding mechanism for a nanoparticle chain waveguide as the transverse resonance of a slot mode between each particle. It is therefore possible to design waveguides that can operate at a specific wavelength, and this can be selected to be in the lower loss regime at wavelengths significantly longer than the plasma resonance. While

we presented a simplified 2D rectangular structure, the same slot mode exists for 3D rectangular nanoparticles, resulting in two resonant dimensions. Furthermore, for other shapes, such as circular cylinders and spheres, a staircase representation for the geometry leads to a series of uniform slot modes, with a similar consequence to the simple case we have described. While there has been much work on scattering from aggregates of nanoparticles, leading to an understanding of scattering and absorption cross sections, and recent studies on nanoparticle chain waveguides, our identification of the role of the slot mode resonance provides both the underlying physical mechanism for an interesting chain waveguide regime and a tool that allows the effective design of waveguides using this principle. The treatment we provide can be extended to 3D, and the influence of a substrate included. As the quality factor of the interparticle space increases with reducing gap, achieving satisfactorily small geometries may be challenging.

This work was supported by the Department of Energy Office of Nonproliferation, Research and Engineering (NA22), in conjunction with Lawrence Livermore National Laboratory, the National Science Foundation (0203240-ECS and 0323037-ECS), and the Army Research Office (DAAD 19-00-1-0387). K.J.W. acknowledges stimulating discussions with G. Barbastathis and D. Psaltis during a 2003 stay at the Massachusetts Institute of Technology.

*Electronic address: webb@purdue.edu

¹M. Quinten, A. Leitner, J. R. Krenn, and F. R. Aussenegg, *Opt. Lett.* **23** (17), 1331 (1998).

²J. R. Krenn, A. Dereux, J. C. Weeber, E. Bourillot, Y. Lacroute, J. P. Goudonnet, G. Schider, W. Gotschy, A. Leitner, F. R. Aussenegg, and C. Girard, *Phys. Rev. Lett.* **82**, 2590 (1999).

³S. A. Maier, M. L. Brongersma, P. G. Kik, and H. A. Atwater, *Phys. Rev. B* **65**, 193408 (2002).

⁴S. A. Maier, P. G. Kik, H. A. Atwater, S. Meltzer, E. Harel, B. E. Koel, and A. A. G. Requicha, *Nat. Mater.* **2**, 229 (2003).

⁵R. Quidant, C. Girard, J. C. Weeber, and A. Dereux, *Phys. Rev. B* **69**, 085407 (2004).

⁶C. Girard, *Rep. Prog. Phys.* **68** (8), 1883 (2005).

⁷S. A. Maier, M. L. Brongersma, and H. A. Atwater, *Appl. Phys. Lett.* **78**, 16 (2001).

⁸P. Ghenuche, R. Quidant, and G. Badenes, *Opt. Lett.* **30** (14), 1882 (2005).

⁹P. B. Johnson and R. W. Christy, *Phys. Rev. B* **6**, 4370 (1972).

¹⁰E. N. Economou, *Phys. Rev.* **182**, 539 (1969).

¹¹W. Rotman, *Proc. IRE* **39**, 952 (1951).